

# Discrete-Time Noise-Suppressing Zhang Neural Network for Dynamic Quadratic Programming with Application to Manipulators

Bolin Liao, and Qihong Xiang

**Abstract**—In this paper, a discrete-time noise-suppressing Zhang neural network (DTNSZNN) model is proposed, analyzed and investigated for the dynamic quadratic programming (QP) subject to dynamic linear-equality constraint. Compared with the discrete-time conventional Zhang neural network (DTCZNN) model or most other conventional methods/algorithms, the DTNSZNN model has the superiority of satisfying the real-time calculation with high precision and suppressing various noises simultaneously. Moreover, relative theoretical analyses are presented for showing the superiority of noise suppressing as well as the high precision. Besides, both the DTCZNN model and the DTNSZNN model are investigated in noise environments and relative numerical experiments are conducted, which further substantiate the efficacy and superiority of the DTNSZNN model in the present of various noises. Furthermore, the DTNSZNN model is applied to robot manipulator motion control to show the feasibility in practice.

**Index Terms**—noise, dynamic quadratic programming, Zhang neural network, discrete-time, real-time calculation.

## I. INTRODUCTION

AS an essential part of nonlinear optimization [1], [2], quadratic programming (QP) is widely studied in engineering fields [3], [4], [5], [6], [7], such as optimal control [3], robotics [4] and classification [5]. In view of its fundamental role, more and more attention has been attached in decades. In [8], the penalty barrier function method was applied for the solution of large-scale QP. In [9], by using a penalty function approach, an exterior point algorithm was developed for convex QP. Note that the computation complexity is normally proportional to the cube of its Hessian matrix's dimension for solving QP, which may be not suitable for high-dimension matrices [10]. Neural network, due to its superiority of parallel-computing and the convenience of hardware implementation, is deeply studied for solving QP problem [11], [12], [13], [14], [15].

However, most neural networks or neural dynamic methods are developed for the static QP problem solving, which is difficult to be employed for the dynamic QP problem solving. Differing from the static (or called time-invariant) QP, the dynamic (or called time-varying) QP has a dynamic

solution instead of a static one, which means that we have to calculate the solution (or say, approximation solution) online. In view of the difficulty of the dynamic QP solving, the relative study is quite few. However, the dynamic QP is often encountered in engineering fields such as robotic control [4], [16]. For solving various dynamic problems effectively, Zhang neural network (ZNN) or Zhang dynamics (ZD), which is a special class of recurrent neural network [17], was proposed by Zhang et al [18], [19]. Zhang neural network opens a door for various dynamic problems solving, such as dynamic nonlinear optimization [20], dynamic Jacobian matrix pseudoinverse [21] and dynamic Sylvester equation [22].

In [23], different types of discrete-time ZNN models were presented for the dynamic equality-constrained dynamic QP. Note that, if the noise is ignored during the calculative process, those discrete-time ZNN models perform well and satisfy the real-time requirement with high precision. However, the noise exists in the real word inevitably and a model ignoring noise is unpractical in practice [24]. In this paper, we propose a discrete-time noise-suppressing ZNN (DTNSZNN) model, which not only satisfies the urgent real-time requirement, but also has the superiority of suppressing different types of noise (i.e., constant noise, bounded random noise and linear noise). For comparison, a discrete-time ZNN model in [23] is also investigated in noise environments, which is named discrete-time conventional ZNN (DTCZNN) model in this paper. Moreover, theoretical analyses are presented to show the stability and convergence of the DTNSZNN model even in the situation of various noises (i.e., constant noise, bounded random noise and linear noise) existing. Note that, in the situation of the constant noise or the bounded random noise existing, the DTNSZNN model shows better performance and has a lower error than the DTCZNN model, and that, in the situation of the linear noise existing, the error of the DTCZNN model increases with the time increasing, while the error of the DTNSZNN model does not, which means that the DTNSZNN model can suppress the linear noise while the DTCZNN model can not.

The remainder of this paper is organized into four sections. Section II introduces the dynamic QP problem and the DTCZNN model. In Section III, we propose the DTNSZNN model and relative theoretical analyses and numerical experiments are presented. In Section IV, the DTNSZNN model is applied to robot manipulator motion planing. Section V concludes this paper with final remarks. Before ending this section, it is worth pointing out here that the main contributions of this paper lie in the following facts.

1) For solving the dynamic QP problem in noise environ-

Manuscript received April 5, 2017; revised August 26, 2017. This work was supported in part by the National Natural Science Foundation of China under Grants 61563017 and 61503152, in part by the Hunan Provincial Natural Science Foundation of China under Grant 2017JJ3258, in part by the Scientific Research Fund of Hunan Provincial Education Department under Grant 17B215, and in part by the Doctoral Scientific Research Foundation of Jishou University under Grant jsdxxcfxbkskyxm201508.

Bolin Liao is with the College of Information Science and Engineering, Jishou University, Jishou 416000, China (corresponding author e-mail: mulinliao8184@163.com).

Qihong Xiang is with College of Mathematics and Statistics, Jishou University, Jishou 416000, China.

ments, the DTNSZNN model is firstly proposed.

- 2) The DTCZNN model in the noise environment is investigated and compared with the DTNSZNN model.
- 3) The efficacy and superiority of the DTNSZNN model are guaranteed by both theoretical analyses and numerical experiments.
- 4) The DTNSZNN model is applied to the robot manipulator control to show the feasibility in practice.

## II. PROBLEM FORMULATION AND DTCZNN MODEL

In this paper, we consider the following problem of dynamic QP subject to dynamic linear-equality constraints [23]:

$$\begin{aligned} \min. \quad & \mathbf{x}^T(t)P(t)\mathbf{x}(t)/2 + \mathbf{q}^T(t)\mathbf{x}(t), \\ \text{sub.} \quad & A(t)\mathbf{x}(t) = \mathbf{b}(t), \end{aligned} \quad (1)$$

where the dynamic decision vector  $\mathbf{x}(t) \in \mathbb{R}^n$  is unknown and is solved for satisfying the above minimization and superscript  $\top$  denotes the transpose of a vector or a matrix. Besides, the Hessian matrix  $P(t) \in \mathbb{R}^{n \times n}$ , the vector  $\mathbf{q}(t) \in \mathbb{R}^n$ , the full-row-rank matrix  $A(t) \in \mathbb{R}^{m \times n}$ , and the vector  $\mathbf{b}(t) \in \mathbb{R}^m$  are all smoothly dynamic. In this paper, we assume that QP (1) is strictly convex, i.e.,  $P(t)$  is positive-definite at any time instant  $t \in [0, \infty)$ . Based on Lagrangian method, dynamic QP problem (1) can be equally converted to the following dynamic linear equations:

$$W(t)\mathbf{y}(t) = \mathbf{u}(t), \quad (2)$$

where

$$\begin{aligned} W(t) &= \begin{bmatrix} P(t) & A^T(t) \\ A(t) & \mathbf{0} \end{bmatrix} \in \mathbb{R}^{(n+m) \times (n+m)}, \\ \mathbf{y}(t) &= \begin{bmatrix} \mathbf{x}(t) \\ \rho(t) \end{bmatrix} \in \mathbb{R}^{n+m}, \quad \mathbf{u}(t) = \begin{bmatrix} -\mathbf{q}(t) \\ \mathbf{b}(t) \end{bmatrix} \in \mathbb{R}^{n+m}, \end{aligned}$$

and  $\rho(t) \in \mathbb{R}^m$  is the Lagrange-multiplier vector.

For solving the dynamic linear equations as well as dynamic QP problem (1), the continuous-time conventional ZNN (CTCZNN) model and the DTCZNN model were proposed by Zhang et al [23]. Specifically, an error function is defined firstly as  $\mathbf{e}(t) = W(t)\mathbf{y}(t) - \mathbf{u}(t)$ . Then, a design formula  $\dot{\mathbf{e}}(t) = -\gamma\mathbf{e}(t)$  is employed to force  $\mathbf{e}(t) \rightarrow \mathbf{0}$  with  $t \rightarrow \infty$ , where  $\gamma > 0$ . Finally, the CTCZNN model is obtained as below:

$$W(t)\dot{\mathbf{y}}(t) = -\dot{W}(t)\mathbf{y}(t) - \gamma(W(t)\mathbf{y}(t) - \mathbf{u}(t)) + \dot{\mathbf{u}}(t). \quad (3)$$

In view of the noise existing, CTCZNN model (3) is rewritten as

$$\begin{aligned} W(t)\dot{\mathbf{y}}(t) &= -\dot{W}(t)\mathbf{y}(t) - \gamma(W(t)\mathbf{y}(t) - \mathbf{u}(t)) \\ &\quad + \dot{\mathbf{u}}(t) + \xi(t), \end{aligned} \quad (4)$$

where  $\xi(t) \in \mathbb{R}^{n \times m}$  denotes the noise, of which the specific value is unknown in calculative processes. Based on CTCZNN model (4) and the Euler method, the following DTCZNN model is obtained:

$$\begin{aligned} \mathbf{y}_{k+1} &= W_k^{-1}(-\tau\dot{W}_k\mathbf{y}_k - h(W_k\mathbf{y}_k - \mathbf{u}_k) + \tau\dot{\mathbf{u}}_k + \tau\xi_k) \\ &\quad + \mathbf{y}_k, \end{aligned} \quad (5)$$

where  $\tau$  is the sampling interval and  $h = \tau\gamma$ ; besides, we denote  $\mathbf{y}_k = \mathbf{y}(t = t_k)$ ,  $W_k = W(t = t_k)$ ,  $\mathbf{y}_k = \mathbf{y}(t = t_k)$

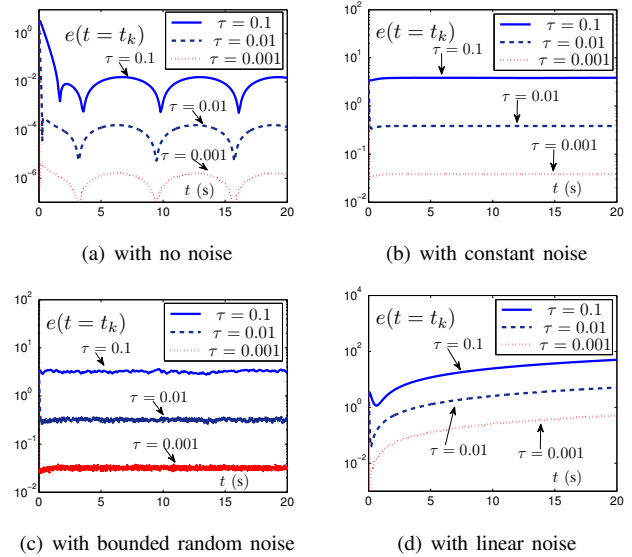


Fig. 1. Order of errors generated by DTCZNN model (5) for solving (6) with different values of  $\tau$  in the different situations

and  $\mathbf{u}_k = \mathbf{u}(t = t_k)$ ;  $W_k^{-1}$  is the inverse of  $W_k$ , and  $t_k$  and  $t_{k+1}$  are continuous time instants where  $k = 0, 1, 2, \dots$ . Note that, if the noise is ignored during the calculative precess, DTCZNN model (5) performs well. Specifically,  $X_{k+1}$  is obtained before time instant  $t_{k+1}$  and we do not need to know the value of  $A_{k+1}$  for calculating  $X_{k+1}$ , which satisfies the urgent real-time requirement. However, the noise is inevitable during the calculative precess and if there exists noise, DTCZNN model (5) may perform not well. For illustrating the above declaration, we conduct some numerical experiments. Let us consider a dynamic QP problem, which is written as the form of (1) with

$$\begin{aligned} P(t) &= \begin{bmatrix} 8 & 2 \exp(-0.5t) \\ 2 \exp(-0.5t) & 10 \end{bmatrix}, \quad \mathbf{q}(t) = \begin{bmatrix} \sin(0.5t) \\ \cos(0.5t) \end{bmatrix}, \\ A(t) &= \begin{bmatrix} 0.8 \exp(-t) \\ 1.5 \end{bmatrix}^T, \quad \text{and} \quad \mathbf{b}(t) = -\cos(0.5t). \end{aligned} \quad (6)$$

In numerical experiments, we set  $h = 0.3$  and  $\tau = 0.1, 0.01$  and  $0.001$ . The error is defined as  $e(t) = e(t = t_k) = \|\mathbf{y}_k - \mathbf{y}_k^*\|_2$ , where  $\mathbf{y}_k^*$  is the theoretical solution which can be calculated by  $\mathbf{y}_k^* = W_k^{-1}\mathbf{u}_k$  and  $\|\cdot\|$  denotes 2-norm of a vector. The results are presented in Fig. 1. From Fig. 1(a), we can observe that, DTCZNN model (5) performs well and the errors generated by DTCZNN model (5) are of order  $10^{-2}$ ,  $10^{-4}$  and  $10^{-6}$  with  $\tau = 0.1, 0.01$  and  $0.001$ , respectively. However, in the present of various noises (i.e., constant noise, bounded random noise and linear noise), model (5) performs not well. Specifically, in the situations of constant and bounded random noises existing, with  $\tau = 0.1$ , the errors generated by model (5) are between 1 and 10, which are relatively large and may not be accepted for the requirement of high calculative precision. In addition, in the situation of the linear noise existing, the error increases with the time increasing.

## III. DTNSZNN MODEL

In view of the weakness of DTCZNN model (5) in the situation of noise existing, we propose the DTNSZNN model

for solving the dynamic linear equations as well as the dynamic QP problem. Moreover, theoretical analyses about the DTNSZNN model are also presented.

### A. Proposing of DTNSZNN model

Before proposing the DTNSZNN model, we present the continuous-time noise-suppressing ZNN (CTNSZNN) model as a basis [24]. Specifically, an error function is defined firstly as  $\mathbf{e}(t) = W(t)\mathbf{y}(t) - \mathbf{u}(t)$ , which is same as previous one and a different design formula  $\dot{\mathbf{e}}(t) = -\lambda_1\mathbf{e}(t) - \lambda_2 \int_0^t \mathbf{e}(\tau)d\tau$  is employed, where  $\lambda_1 > 0$  and  $\lambda_2 > 0$ . Then, the following CTNSZNN model in the situation of the noise existing is obtained:

$$W(t)\dot{\mathbf{y}}(t) = -\dot{W}(t)\mathbf{y}(t) - \lambda_1(W(t)\mathbf{y}(t) - \mathbf{u}(t)) + \dot{\mathbf{u}}(t) - \lambda_2 \left( \int_0^t W(\tau)\mathbf{y}(\tau) - \mathbf{u}(\tau)d\tau \right) + \xi(t). \quad (7)$$

Based on the following lemmas, the convergence of CTNSZNN model (7) in different situations (i.e., with no noise, constant noise, bounded random noise and linear noise) is guaranteed [24].

*Lemma 1:* With no noise existing during the calculative process, CTNSZNN model (7) converges to the theoretical solution of problem (1) with the steady-state error (SSE) (i.e.,  $\lim_{t \rightarrow \infty} \|W(t)\mathbf{y}(t) - \mathbf{u}(t)\|_2$ ) being zero.

*Lemma 2:* In the situation of three different types of noise existing, CTNSZNN model (7) is convergent: 1) with the constant noise existing, CTNSZNN model (7) converges to the theoretical solution with the SSE being 0; 2) with the bounded random noise existing, CTNSZNN model (7) converges to the theoretical solution with the SSE being bounded and approximately in inverse proportion to  $\lambda_1$ ; 3) with the linear noise existing, CTNSZNN model (7) converges to the theoretical solution with the SSE being bounded and in inverse proportion to  $\lambda_2$ ;

Focusing on CTNSZNN model (7), we can observe that model (7) may not be discretized directly by the Euler method or other discretization formulas due to the existence of the integral term  $\int_0^t W(\tau)\mathbf{y}(\tau) - \mathbf{u}(\tau)d\tau$ . For solving this problem, we define  $\mathbf{z}(t) = \int_0^t W(\tau)\mathbf{y}(\tau) - \mathbf{u}(\tau)d\tau$  and model (7) can be rewritten as the following form:

$$\begin{cases} \dot{\mathbf{y}}(t) = W(t)^{-1} \left( -\dot{W}(t)\mathbf{y}(t) - \lambda_1(W(t)\mathbf{y}(t) - \mathbf{u}(t)) + \dot{\mathbf{u}}(t) - \lambda_2\mathbf{z}(t) + \xi(t) \right) \\ \dot{\mathbf{z}}(t) = W(t)\mathbf{y}(t) - \mathbf{u}(t). \end{cases} \quad (8)$$

We use the Euler method [23], [25] to discretize the terms  $\dot{\mathbf{y}}(t)$  and  $\dot{\mathbf{z}}(t)$  of the above CTNSZNN model (8) simultaneously, and the following DTNSZNN model is obtained:

$$\begin{cases} \mathbf{y}_{k+1} = W_k^{-1} \left( -\tau\dot{W}_k\mathbf{y}_k - \kappa_1(W_k\mathbf{y}_k - \mathbf{u}_k) + \tau\dot{\mathbf{u}}_k - \kappa_2\mathbf{z}_k + \tau\xi_k \right) + \mathbf{y}_k \\ \mathbf{z}_{k+1} = \tau(W_k\mathbf{y}_k - \mathbf{u}_k) + \mathbf{z}_k, \end{cases} \quad (9)$$

where parameters  $\kappa_1 = \gamma_1\tau$  and  $\kappa_2 = \gamma_2\tau$ . Note that we may use other discretization formulas to discretize the CTNSZNN model, and then obtain different discrete-time ZNN models. Specifically, we may use the Taylor-Type discretization formula which is employed in [23]. We know that the truncation error of Taylor-Type discretization formula is

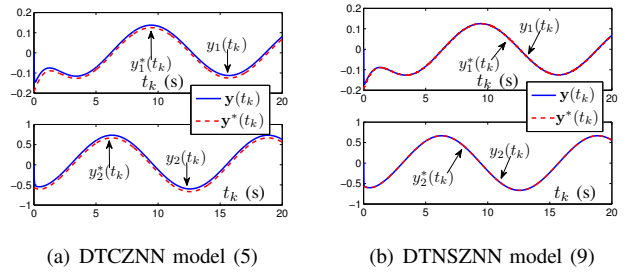


Fig. 2. Solution states of DTCZNN model (5) and DTNSZNN model (9) with constant noise, where solid lines and dashed lines denote calculated solution states  $\mathbf{y}(t_k)$  and theoretical solution states  $\mathbf{y}^*(t_k)$ , respectively

$O(\tau^2)$ , which is higher than that of Euler method. However, from the theoretical analyses in the ensuing subsection, we can find that, due to the limitation of calculative precision of CTNSZNN model (7), we cannot get a higher calculative precision for DTNSZNN model (9) in the present of the bounded random noise or the linear noise. Besides, higher calculative precision of discretization formula means higher time and space costs.

### B. Theoretical analyses of DTNSZNN model

In this subsection, theoretical analyses are presented for showing the convergence of DTNSZNN model (9) and the superiority in the situation of various noises existing.

*Proposition 1:* In terms of the dynamic QP problem (1), considering the situation that no noise exists during the calculative process, DTNSZNN model (9) converges to the theoretical solution with the discrete-time SSE (i.e.,  $\lim_{k \rightarrow \infty} \|\mathbf{y}_k - \mathbf{y}_k^*\|_2$ ) being  $O(\tau^2)$ .

*Proof.* According to Definition 1 in Appendix A, the characteristic polynomial of DTNSZNN model (9) can be derived as

$$P(\theta) = \theta - 1, \quad (10)$$

which has only one root, i.e.,  $\theta_1 = 1$ , which is on the unit circle, so DTNSZNN model (9) is 0-stable considering no bias noise existing. In addition, we know that the SSE of DTNSZNN model (9) is 0 from Lemma 1, and that the truncation error of Euler method is  $O(\tau)$ . Therefore, we have the following equation:

$$\begin{cases} \mathbf{y}_{k+1} = W_k^{-1} \left( -\tau\dot{W}_k\mathbf{y}_k - \kappa_1(W_k\mathbf{y}_k - \mathbf{u}_k) + \tau\dot{\mathbf{u}}_k - \kappa_2\mathbf{z}_k \right) + \mathbf{y}_k + \mathbf{O}(\tau^2) \\ \mathbf{z}_{k+1} = \tau(W_k\mathbf{y}_k - \mathbf{u}_k) + \mathbf{z}_k + \mathbf{O}(\tau^2), \end{cases}$$

where  $\mathbf{O}(\tau^2)$  denotes a vector with every elements being  $O(\tau^2)$ . Then, according to Definition 3 in Appendix, it can be derived that DTNSZNN model (9) is consistent and convergent, which converges with the order of its truncation error being  $\mathbf{O}(\tau^2)$ . From the above analysis, it can be concluded that  $\mathbf{y}_k = \mathbf{y}_k^* + \mathbf{O}(\tau^2)$  with  $k$  large enough. Therefore,

$$\begin{aligned} \|W_k\mathbf{y}_k - \mathbf{u}_k\|_2 &= \|W_k(\mathbf{y}_k^* + \mathbf{O}(\tau^2)) - \mathbf{u}_k\|_2 \\ &= \|W_k\mathbf{O}(\tau^2)\|_2 = O(\tau^2). \end{aligned}$$

The proof is thus completed.  $\square$

*Proposition 2:* In terms of the dynamic QP problem (1), considering the situation that different types of noises exist

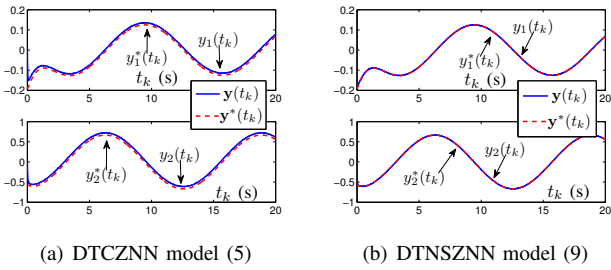


Fig. 3. Solution states of DTCZNN model (5) and DTNSZNN model (9) with random noise, where solid lines and dashed lines denote calculated solution states  $\mathbf{y}(t_k)$  and theoretical solution states  $\mathbf{y}^*(t_k)$ , respectively

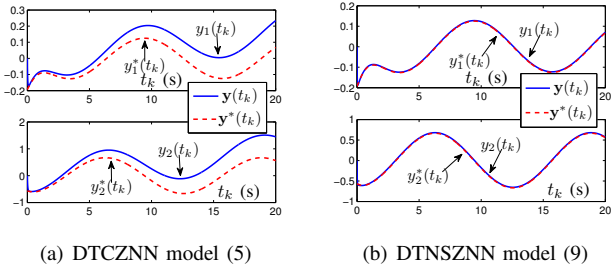


Fig. 4. Solution states of DTCZNN model (5) and DTNSZNN model (9) with linear noise, where solid lines and dashed lines denote calculated solution states  $\mathbf{y}(t_k)$  and theoretical solution states  $\mathbf{y}^*(t_k)$ , respectively

during the calculative process, DTNSZNN model (9) converges the theoretical solution with different discrete-time SSEs as below. 1) For the constant noise, the discrete-time SSE is  $O(\tau^2)$ ; 2) for the bounded random noise, if  $\kappa_1$  is unaltered, the discrete-time SSE is approximately  $O(\tau)$ ; 3) for the linear noise, if  $\kappa_2$  is unaltered, the discrete-time SSE is  $O(\tau)$ .

*Proof.* The proof process can be divided into three parts as below.

1) For the constant noise, the proof process is similar to that of Proposition 1 and thus is omitted here.

2) For the bounded random noise, according to Definition 1 in Appendix, we know that DTNSZNN model (9) is 0-stable. From Lemma 2, we know that CTNSZNN model (7) converges to the theoretical solution of (1) with the SSE is approximately in inverse proportion to  $\lambda_1$  i.e., the SSE is approximately  $O(1/\lambda_1)$ . In addition, we know that  $\tau\lambda_1 = \kappa_1$  in DTNSZNN model (9). Thus, if the value of  $\kappa_1$  is unaltered,  $\tau$  is in inverse proportion to  $\gamma_1$ , i.e.,  $\tau = \kappa_1/\gamma_1$ . Besides, the calculative precision of Euler method is  $O(\tau)$ . Thus, if the value of  $\kappa_1$  is unaltered, we have that

$$\begin{cases} \mathbf{y}_{k+1} = \mathbf{W}_k^{-1}(-\tau\dot{\mathbf{W}}_k\mathbf{y}_k - \kappa_1(\mathbf{W}_k\mathbf{y}_k - \mathbf{u}_k) + \tau\dot{\mathbf{u}}_k \\ \quad - \kappa_2\mathbf{z}_k + \tau\xi_k) + \mathbf{y}_k + \mathbf{O}(\tau) \\ \mathbf{z}_{k+1} = \tau(\mathbf{W}_k\mathbf{y}_k - \mathbf{u}_k) + \mathbf{z}_k + \mathbf{O}(\tau). \end{cases}$$

Then, according to Definitions 2 and 3, the convergence of DTNSZNN model (9) is ensured. From the above analysis, it can be concluded that  $\mathbf{y}_k = \mathbf{y}_k^* + \mathbf{O}(\tau)$  with  $k$  large enough. Therefore,

$$\begin{aligned} \|\mathbf{W}_k\mathbf{y}_k - \mathbf{u}_k\|_2 &= \|\mathbf{W}_k(\mathbf{y}_k^* + \mathbf{O}(\tau)) - \mathbf{u}_k\|_2 \\ &= \|\mathbf{W}_k\mathbf{O}(\tau)\|_2 = O(\tau). \end{aligned}$$

3) For the linear noise, the proof process is similar to that of the bounded random noise and thus is omitted here. The proof is thus completed.  $\square$

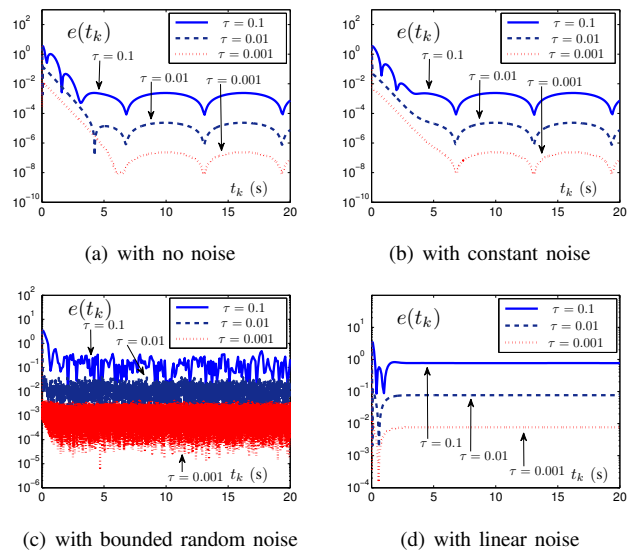


Fig. 5. Order of errors generated by DTNSZNN model (9) for solving (6) with different values of  $\tau$  in the different situations

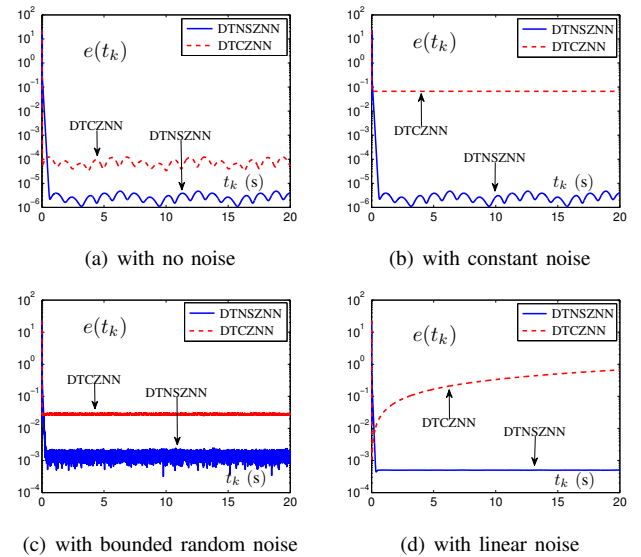


Fig. 6. Errors generated by DTNSZNN model (9) and DTCZNN model (5) for solving (11)-(14) in the different situations with  $\tau = 0.001$

### C. Numerical verifications

In this subsection, some numerical experiments are conducted to verify the efficacy and the superiority of DTNSZNN model (9) for solving the dynamic QP problem (1) considering the situation that three types of noises exist. For comparison, the specific dynamic QP problem (6), which is investigated in Section II for showing the weakness of DTCZNN model (5), is investigated again. In numerical experiments, we set  $\kappa_1 = 0.5$  and  $\kappa_2 = 1$ . Note that parameters  $\kappa_1$  and  $\kappa_2$  are selected relatively freely in appropriate ranges.

For showing the superiority of DTNSZNN model (9) compared with DTCZNN model (5), a series of numerical experiments are conducted and the results are displayed in Fig. 2 through Fig. 4, where solid curves correspond to the solution elements, and the dash-dotted curves correspond to the theoretical solution elements. In these numerical experiments, we set  $\tau = 0.01$ . From Fig. 2 and Fig. 3,



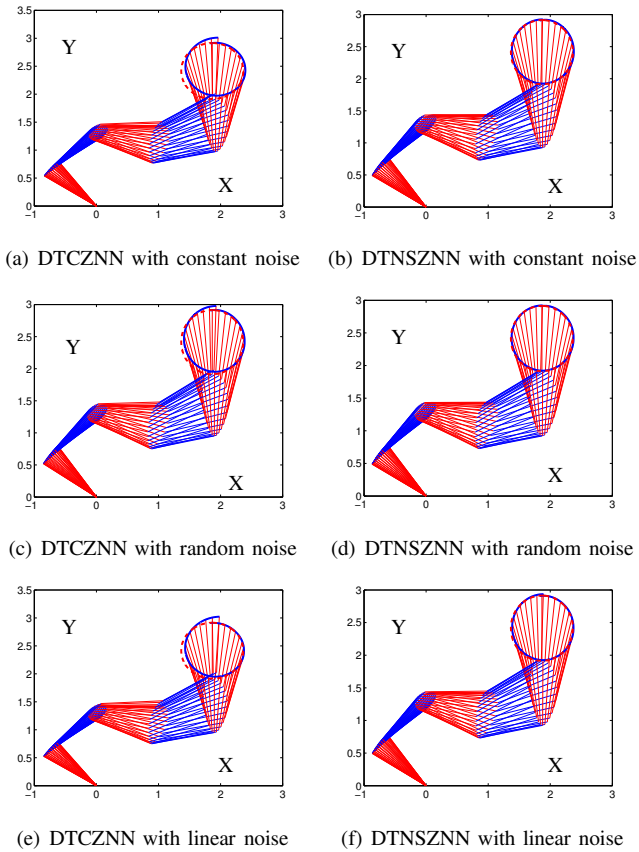


Fig. 7. Motion trajectories of planar robot manipulator generated by DTCZNN and DTNSZNN models with various kinds of noises.

one can observe that DTNSZNN model (9) performs much better than DTCZNN model (5). Moreover, Fig. 4 shows that DTNSZNN model (9) can suppress the linear noise and the actual solution overlaps the theoretical solution during the whole calculative process. In contrast, DTCZNN model (5) cannot suppress linear noise and the error generated by DTCZNN model (5) increases with the time increasing.

For further substantiating the calculative precision of DTNSZNN model (9) which is shown in the above subsection, some numerical experiments are conducted and the results are plotted in Fig. 5. From Fig. 5(a), it can be observed that, with  $\tau = 0.1, 0.01$  or  $0.001$ , the discrete-time SSE are of order  $10^{-2}, 10^{-4}$  or  $10^{-6}$ , which substantiates that DTNSZNN model (9) with no noise converges the theoretical solution with the discrete-time SSE being  $O(\tau^2)$ . Similar to Fig. 5(a), Fig. 5(b) shows that DTNSZNN model (9) with the constant noise converges the theoretical solution with the discrete-time SSE being  $O(\tau^2)$ . It follows from Fig. 5(c) and Fig. 5(d) that, with  $\tau = 0.1, 0.01$  or  $0.001$ , the discrete-time SSEs are both of order  $10^{-1}, 10^{-2}$  or  $10^{-3}$ , which substantiates that DTNSZNN model (9) with the bounded random noise or the linear noise converges the theoretical solution with the discrete-time SSE being  $O(\tau)$ .

To substantiate the effectiveness and superiority of DTNSZNN model (9) to solve more complicated dynamic QP problems, we consider complicated one, which is rewritten

as the form of (1) with

$$P(t) = \begin{bmatrix} p_1(t) & p_2(t) & p_3(t) & \cdots & p_n(t) \\ p_2(t) & p_1(t) & p_2(t) & \cdots & p_{n-1}(t) \\ p_3(t) & p_2(t) & p_1(t) & \cdots & p_{n-2}(t) \\ \vdots & \vdots & \vdots & \cdots & \vdots \\ p_n(t) & p_{n-1}(t) & p_{n-2}(t) & \cdots & p_1(t) \end{bmatrix} \quad (11)$$

where  $p_1(t) = 8 + \cos(t)$ , and  $p_i(t) = \sin(t)/(i-1)$  with  $i = 2, 3, \dots, n$ . Besides, the other coefficients of QP problem (1) are as below:

$$\mathbf{q}(t) = [-2 \cos(2t), 2 \cos(2t + \pi/2), 2 \cos(2t + \pi), \dots, 2 \cos(2t + (n-1)\pi/2)]^T \quad (12)$$

$$A(t) = [\sin(t), \sin(t - \pi/3), \sin(t - 2\pi/3), \dots, \sin(t - (n-1)\pi/3)] \quad (13)$$

and

$$\mathbf{b}(t) = [2 \cos(2t + n\pi/2)]. \quad (14)$$

In numerical experiments, we set  $n = 6$ , and sampling gap  $\tau = 0.001$ . We consider a constant noise vector with each element being 20. Besides, a bounded random noise vector with each element randomly changing from 7 to 9 and a linear increasing noise vector with each element being  $10t_k$  are also considered. Numerical experimental results are presented in Fig. 6. It is evident that, in all different situations, DTNSZNN model (9) is superior to DTCZNN model (5).

#### IV. APPLICATION TO ROBOT MANIPULATORS

In this section, DTNSZNN model (9) is applied to the motion control of robot manipulators [26], [27], [28] with various noises. Besides, DTCZNN model (5) is also applied to such a task to show the superiority of DTNSZNN model (9).

In this application, a 5-link planar robot manipulator is considered and investigated with its forward-kinematics equation being

$$\psi(\epsilon(t)) = \varrho(t), \quad (15)$$

where  $\psi(\cdot)$  is the forward-kinematics mapping function with known structure and parameters for a given manipulator. In addition,  $\epsilon(t) \in \mathbb{R}^5$  and  $\varrho(t) \in \mathbb{R}^2$  denote the joint-angle vector and the end-effector Cartesian position vector, respectively. By differentiating the both sides of (15), the following equation is obtained:

$$J(\epsilon(t))\dot{\epsilon}(t) = \dot{\varrho}(t), \quad (16)$$

where matrix  $J(\epsilon(t)) = \partial\psi(\epsilon(t))/\partial\epsilon(t) \in \mathbb{R}^{2 \times 5}$ ;  $\dot{\varrho}(t)$  denotes the Cartesian velocity; and  $\dot{\epsilon}(t)$  denotes the joint velocity. The robot manipulator is investigated to track a circle path with the radius being 0.5 m with various kinks of noises considered. At the same time, the joint velocity should be minimized. Thus, the control problem is formulated as

$$\begin{aligned} \min. \quad & \dot{\epsilon}^T(t)\dot{\epsilon}(t), \\ \text{sub.} \quad & J(\epsilon(t))\dot{\epsilon}(t) = \dot{\varrho}(t), \end{aligned} \quad (17)$$

DTNSZNN model (9) and DTCZNN model (5) are employed to solve this problem. The task duration  $T = 10$  s; each link length is 1 m;  $\tau = 0.001$  s; initial joint state  $\epsilon_0 = [3\pi/4, -\pi/2, -\pi/4, \pi/6, \pi/3]$  rad. Numerical results

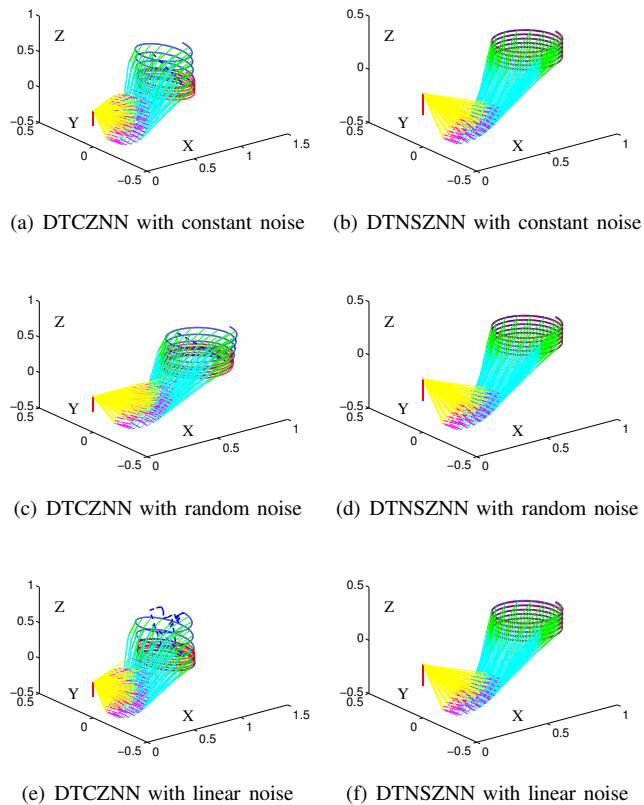


Fig. 8. Motion trajectories of PUMA560 robot manipulator generated by DTCZNN and DTNSZNN models with various kinds of noises.

are presented in Fig. 7. It is evident that DTNSZNN model (9) is superior to DTCZNN model (5) with three different kinds of noises, i.e., constant noise, random noise and linear noise.

Moreover, DTNSZNN model (9) is applied to the motion control of PUMA560 robot manipulator [28] with various noises, which is a 3D robot manipulator. Besides, DTCZNN model (5) is also applied to such a task. Numerical results are presented in Fig. 8, which substantiate the superiority of DTNSZNN model (9) once again.

## V. CONCLUSION

In this paper, the DTNSZNN model has been proposed for solving the dynamic QP problem. Note that the DTNSZNN model not only has the advantage of satisfying the urgent real-time computation, but also has the advantage of suppressing various noise (i.e., the constant noise, the bounded random noise and the linear noise). Theoretical analyses have been presented for showing the stability and convergence of the proposed model. Theoretical results have shown that, in the situation of various noises existing, DTNSZNN model performs well and has a relatively high calculative precision. Moreover, comparative numerical experiments and applications have been conducted for further substantiating the efficacy and superiority of the proposed DTNSZNN model.

## APPENDIX

**Definition 1:** An  $N$  step method  $\sum_{j=0}^N \alpha_j x_{k+j} = g \sum_{j=0}^N \beta_j f_{k+j}$  can be checked for 0-stability by determining the roots of characteristic polynomial  $P_N(\theta) =$

$\sum_{j=0}^N \alpha_j \theta^j$ . If the roots of  $P_N(\theta) = 0$  are such that  $|\theta| \leq 1$  and those for which  $|\theta| = 1$  are simple, then the  $N$  step method is 0-stable.

**Definition 2:** An  $N$  step method is said to be consistent of order  $p$  if its truncation error is  $O(g^p)$  with  $p > 0$  for the smooth exact solution.

**Definition 3:** An  $N$  step method is convergent, i.e.,  $x_{[(t-t_0)/g]} \rightarrow x^*(t)$ , for all  $t \in [t_0, t_{\text{final}}]$ , as  $g \rightarrow 0$ , if and only if the method is 0-stable and consistent. That is to say, 0-stability plus consistency results in convergence. In particular, a 0-stable consistent method converges with the order of its truncation error.

## REFERENCES

- [1] J. Wang and J. Song, "A hybrid algorithm based on gravitational search and particle swarm optimization algorithm to solve function optimization problems," *Engineering Letters*, vol. 25, no. 1, pp. 22–29, 2017.
- [2] O. Castillo, E. Rubio, J. Soria, and E. Naredo, "Optimization of the fuzzy C-Means algorithm using evolutionary methods," *Engineering Letters*, vol. 20, no. 1, pp. 61–67.
- [3] D. Jin and H. Hu, "Optimal control of a tethered subsatellite of three degrees of freedom," *Nonlinear Dynamics*, vol. 46, no. 1, pp. 161–178, 2006.
- [4] D. Guo and Y. Zhang, "New inequality-based obstacle-avoidance MVN scheme and its application to redundant robot manipulators," *Systems Man & Cybernetics, IEEE Transactions on*, vol. 42, no. 6, pp. 1326–1340, 2012.
- [5] Q. Liu, "Kernel local sparse representation based classifier," *Neural Processing Letters*, vol. 43, no. 1, pp. 85–95, 2016.
- [6] K. Ramesh, A. Hisyam, N. Aziz, and S. R. A. Shukor, "Nonlinear model predictive control of a distillation column using wavenet based Hammerstein model," *Engineering Letters*, vol. 20, no. 4, pp. 330–335, 2012.
- [7] R. S. Schittenhelm, Z. Wang, B. Riemann, and S. Rinderknecht, "State feedback in the context of a gyroscopic rotor using a disturbance observer," *Engineering Letters*, vol. 21, no. 1, pp. 44–51, 2013.
- [8] V. S. Vassiliadis, "Application of the modified barrier method in large-scale quadratic programming problems," *Computers & Chemical Engineering*, vol. 20, pp. 243–248, 1996.
- [9] M. Ben-Daya and K. S. Al-Sultan, "A new penalty function algorithm for convex quadratic programming," *European Journal of Operational Research*, vol. 101, no. 1, pp. 155–163, 1997.
- [10] Y. Zhang and Z. Li, "Zhang neural network for online solution of dynamic convex quadratic program subject to dynamic linear-equality constraints," *Physics Letters A*, vol. 373, no. 18–19, pp. 1639–1643, 2009.
- [11] S. Li, Y. Li, and Z. Wang, "A class of finite-time dual neural networks for solving quadratic programming problems and its k-winners-take-all application," *Neural Networks*, vol. 39, pp. 27–39, 2013.
- [12] Y. Chen, C. Yi, and J. Zhong, "Linear simultaneous equations' neural solution and its application to convex quadratic programming with equality-constraint," *Journal of Applied Mathematics*, vol. 2013, no. 5, pp. 1–6, 2013.
- [13] P. Miao, Y. Shen, and X. Xia, "Finite time dual neural networks with a tunable activation function for solving quadratic programming problems and its application," *Neurocomputing*, vol. 143, pp. 80–89, 2014.
- [14] C. Sha, H. Zhao, and F. Ren, "A new delayed projection neural network for solving quadratic programming problems with equality and inequality," *Neurocomputing*, vol. 168, pp. 1164–1172, 2015.
- [15] L. Jin, S. Li, L. Xiao, R. Lu, and B. Liao, "Cooperative motion generation in a distributed network of redundant robot manipulators with noises," *Systems, Man, and Cybernetics: Systems, IEEE Transactions on*, In Press with DOI 10.1109/TSMC.2017.2693400.
- [16] L. Xiao and Y. Zhang, "Solving time-varying inverse kinematics problem of wheeled mobile manipulators using Zhang neural network with exponential convergence," *Nonlinear Dynamics*, vol. 76, no. 2, pp. 1543–1559, 2014.
- [17] L. Yang, Y. Yang, Y. Li, and T. Zhang, "Almost periodic solution for a Lotka-Volterra recurrent neural networks with harvesting terms on time scales," *Engineering Letters*, vol. 24, no. 4, pp. 455–460, 2016.
- [18] Y. Zhang and S. Ge, "Design and analysis of a general recurrent neural network model for dynamic matrix inversion," *Neural Networks, IEEE Transactions on*, vol. 16, no. 6, pp. 1477–1490, 2005.

- [19] D. Guo and Y. Zhang, "Zhang neural network for online solution of time-varying linear matrix inequality aided with an equality conversion," *Neural Networks and Learning Systems, IEEE Transactions on*, vol. 25, no. 2, pp. 370–382, 2014.
- [20] L. Jin and Y. Zhang, "Continuous and discrete Zhang dynamics for real-time varying nonlinear optimization," *Numerical Algorithms*, vol. 73, no. 1, pp. 115–140, 2016.
- [21] L. Xiao and Y. Zhang, "From different Zhang functions to various ZNN models accelerated to finite-time convergence for time-varying linear matrix equation," *Neural Processing Letters*, vol. 39, no. 3, pp. 309–326, 2014.
- [22] S. Li, S. Chen, and B. Liu, "Accelerating a recurrent neural network to finite-time convergence for solving time-varying Sylvester equation by using a sign-bi-power activation function," *Neural Processing Letters*, vol. 37, no. 2, pp. 189–205, 2013.
- [23] B. Liao, Y. Zhang, and L. Jin, "Taylor  $O(h^3)$  discretization of ZNN models for dynamic equality-constrained quadratic programming with application to manipulators," *Neural Networks and Learning Systems, IEEE Transactions on*, vol. 27, no. 2, pp. 225–237, 2016.
- [24] L. Jin, Y. Zhang, and S. Li, "Integration-enhanced Zhang neural network for real-dynamic matrix inversion in the presence of various kinds of noises," *Neural Networks and Learning Systems, IEEE Transactions on*, vol. 27, no. 12, pp. 2615–2627, 2016.
- [25] D. F. Griffiths and D. J. Higham, *Numerical Methods for Ordinary Differential Equations: Initial Value Problems*. Springer-Verlag, London, 2010.
- [26] J. Zhang, L. Yu, and L. Ding, "Velocity feedback control of swing phase for 2-DoF robotic leg driven by electro-hydraulic servo system," *Engineering Letters*, vol. 24, no. 4, pp. 378–383, 2016.
- [27] R. M. Mahamood, "Improving the performance of adaptive PDPID control of two-link flexible robotic manipulator with ILC," *Engineering Letters*, vol. 20, no. 3, pp. 259–270, 2012.
- [28] B. Cai and Y. Zhang, "Bi-criteria optimal control of redundant robot manipulators using LVI-based primal-dual neural network," *Optimal Control Applications and Methods*, vol. 31, no. 3, pp. 213–229, 2010.

**B. Liao** was born in Hunan, China, in 1981. He received the Ph.D. degree in communication and information systems from Sun Yat-Sen University, Guangzhou, China, in 2015. He is currently an Associate Professor with the College of Information Science and Engineering, Jishou University. His current research interests include neural networks, robotics and nonlinear control. He has published around 50 papers in various journals/conferences.